Radiation Measurements 114 (2018) 8–11

Contents lists available at ScienceDirect

Radiation Measurements

journal homepage: www.elsevier.com/locate/radmeas

Experimental study on fluence rate response of $LaBr_3$ to pulsed X-rays

Yicheng Yi[a,*], Zhaohui Song[a,b], Lu Yi[a], Xingyin Guan[a], Xiang Chen[a], Gang Li[a], Kan Zhang[a]

[a] Northwest Institute of Nuclear Technology, Xi'an 710024, China
[b] State Key Laboratory of Intense Pulsed Radiation Simulation and Effect, Xi'an 710024, China

ARTICLE INFO

Keywords:
$LaBr_3$ scintillator
Linear response limit
Lissajous figure
Fluence rate

ABSTRACT

The linear response is the key property employed by a radiation detector to determine the accurate intensity of a pulse radiation field. In this study, we investigated the high fluence rate response behavior of a $LaBr_3$ scintillator. We used a high-intensity pulsed X-ray source called "QiangGuang-I" which could produce an X-ray pulse with a total dose of 100 Gy, full width at half maximum of 20 ± 5 ns, and an average energy of 1 MeV, to test the linear response of the $LaBr_3$ scintillator. The Lissajous figure method was used in this experiment. The results showed that the fluence rate linear response limit was more than 1.8×10^{20} MeV/(cm^2·s).

1. Introduction

Lanthanum bromide mixed with Ce^{3+} ($LaBr_3$:Ce^{3+}) scintillators discovered at Delft University of Technology and the University of Bern have been studied extensively in recent years. $LaBr_3$ scintillators have superior properties such as high energy resolution (2.9% for 662 keV gamma rays), fast response time (typically ~22 ns), small non-proportionality (< 6% for 30 keV-1000 keV gamma rays), and high scintillation yield (~60,000 ph/MeV for Φ50 mm × 50 mm $LaBr_3$ scintillator) (Van Loef et al., 2001, 2002; Krämer et al., 2006; Glodo et al., 2005). $LaBr_3$ detectors are also promising for measuring the intensity of pulsed X-rays in a mixed X/neutron field because of their fast rising time and high gamma/neutron discrimination (Lu et al., 2014).

In this study, we evaluated the high fluence rate response behavior of a $LaBr_3$ scintillator. The mechanism of this nonlinear response is complex and the fluence rate linear response limit cannot be derived by simulation. This parameter can only be acquired using experimental methods.

2. Experimental conditions and method

The pulsed power accelerator called "QiangGuang-1" was used to provide a high fluence rate pulsed X-ray radiation field. The X-ray generation process was introduced below. High voltage pulse was produced by a linear transformer driver. After twice pulse compression, great electrical current pulse was collected on the load. The discharge process of electrical currents was controlled by a plasma opening switch. High energy electron beam was produced then. The bremsstrahlung X-ray was generated by the collision of high energy electron beam and tantalum targets.

The full width at half maximum (FWHM) of the pulsed X-ray was about 15–25 ns and the maximum dose near the target was higher than 100 Gy. The pulsed X-ray emission spectroscopy of "QiangGuang-1" accelerator was shown in Fig. 1. The average X-ray energy was approximately 1 MeV (Cong et al., 2010). This pulsed radiation facility is ideal for studying the high fluence rate response behavior of radiation detectors (Song et al., 2004).

The experimental layout is shown in Fig. 2. The detector placed near the target is called the former detector. The detector located further from the target is called the latter detector, which is always operated in the linear response mode in this study. Each detector comprised one $LaBr_3$ scintillator measuring 50 mm × 10 mm (produced by Saint-Gobain in 2015) and one photoelectric tube (GD40).

In order to avoid the GD40 tube in the former detector being directly irradiated, the former detector was set as shown in Fig. 3. Lead bricks with a thickness of 20 cm were placed in a position between the target and the former detector. The latter detector was set at a certain distance (> 3 m) where the noise caused by direct X rays can be neglected.

The linear current of the GD40 in the former detector was tested by a pulse xenon lamp. The results were shown in Fig. 4. Fig. 4 (b) showed the linear output upper of the GD40 is nearly 9.5 V. The attenuation of the GD40 is 40 dB. The channel resistance of the oscilloscope was 50 Ω. The linear current $I_{\max}$ of the GD40 is

$$I_{\max} = \frac{V_{\max} \times 100}{R_{channel}} = \frac{9.5\ \text{V} \times 100}{50\ \Omega} = 19\ \text{A}$$

A digital oscilloscope was used to record the output curves from the

* Corresponding author.
E-mail address: yiyicheng@nint.ac.cn (Y. Yi).

https://doi.org/10.1016/j.radmeas.2018.04.012
Received 18 July 2017; Received in revised form 17 April 2018; Accepted 19 April 2018
Available online 23 April 2018
1350-4487/

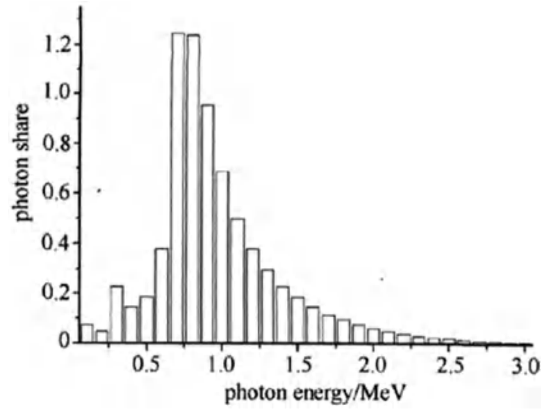

Fig. 1. X-ray emission spectroscopy of "QiangGuang-1" accelerator (Cong et al., 2010).

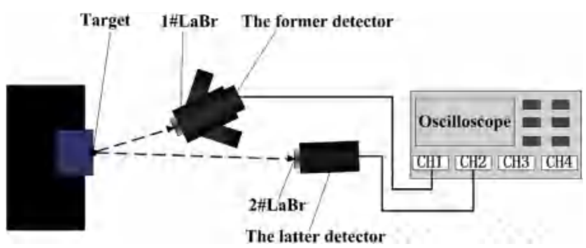

Fig. 2. Experimental layout.

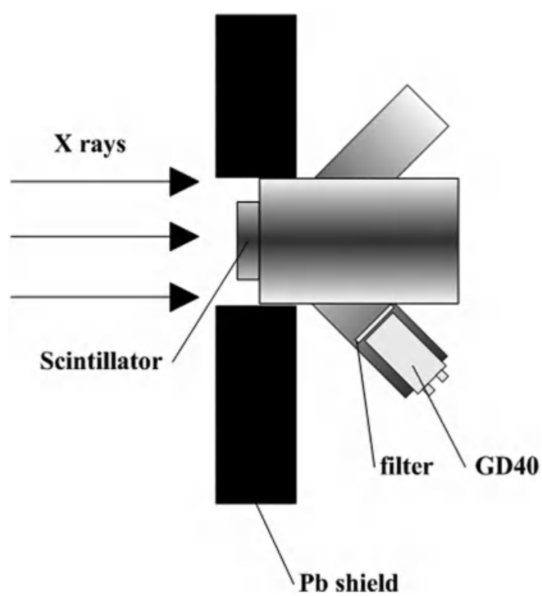

Fig. 3. The former detector.

two detectors. The channel resistance of the oscilloscope was 50 Ω. Considering the outputs of the detectors could exceed the range of the oscilloscope at high dose rates, the signals were attenuated and subjected to power dividers before they were imported into the oscilloscope (as shown in Table 1).

The dose that entered the $LaBr_3$ detector in each pulse was monitored using three LiF(Mg)-M thermo luminescent dosimeter (TLD) chips placed on the front surfaces of the detectors. The linearity range of the TLD chips is 5×10^{-5} Gy to 500 Gy. The uncertainty of the dose measurement was 25.1% (Cong et al., 2010). The pulse width was monitored by a Si-PIN detector (Kuckuck RW, 1971; Kun-Sik Park., 2006; Guo et al., 2014). The parameters of the detector were shown in Table 2.

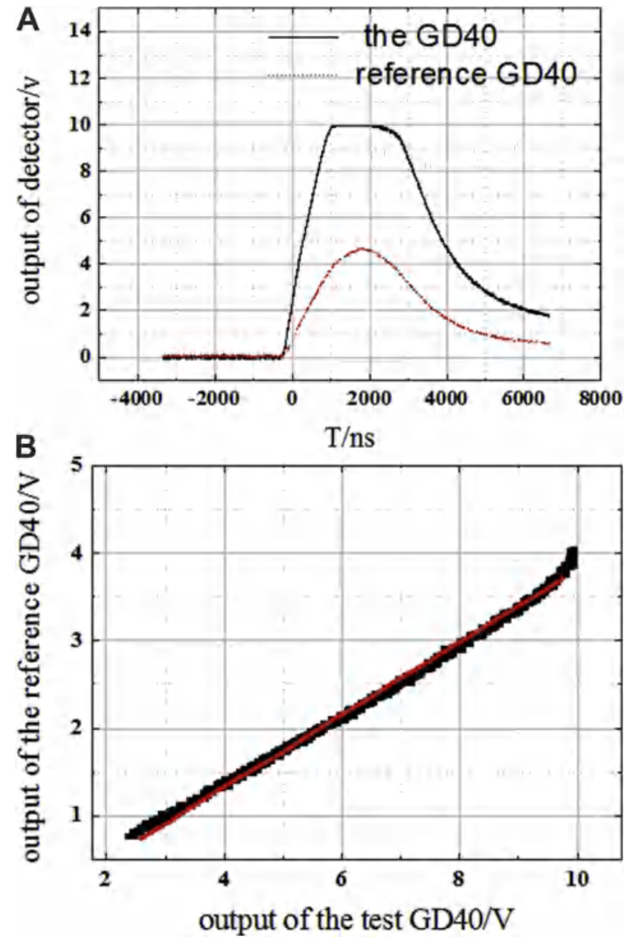

Fig. 4. Measurement of the maximum pulse linear current of the GD40.

Table 1
Attenuation and power dividers properties of detectors.

	The former detector				The latter detector			
Filter	10%				50%			
Divided factor	4				4			
attenuation	None	6 dB	20 dB	30 dB	None	10 dB	20 dB	30 dB
V/div	1 V	1 V	1 V	1 V	1 V	1 V	500 mV	500 mV

Table 2
The parameters of the Si-PIN detector.

Size/mm	Energy response range/MeV	Working voltage/V	Rise time/ns	FWHM/ns
Φ12*0.3	0.8–8.0	−800 ± 15	1.15	2.39

3. Results and discussion

3.1. Results

Fig. 5(a) shows the output waveforms for the detectors in the first X-ray shot. The amplitudes of the waveforms obtained by the former detector are shown on the X-axis and that for the latter detector on the Y-axis in the Lissajous figure in Fig. 5(b). There was a linear relationship between the amplitudes of the former and the latter detectors, which indicated that the 1#$LaBr_3$ scintillator exhibited a linear response. The dose that entered the front detector was 21.06 Gy and the

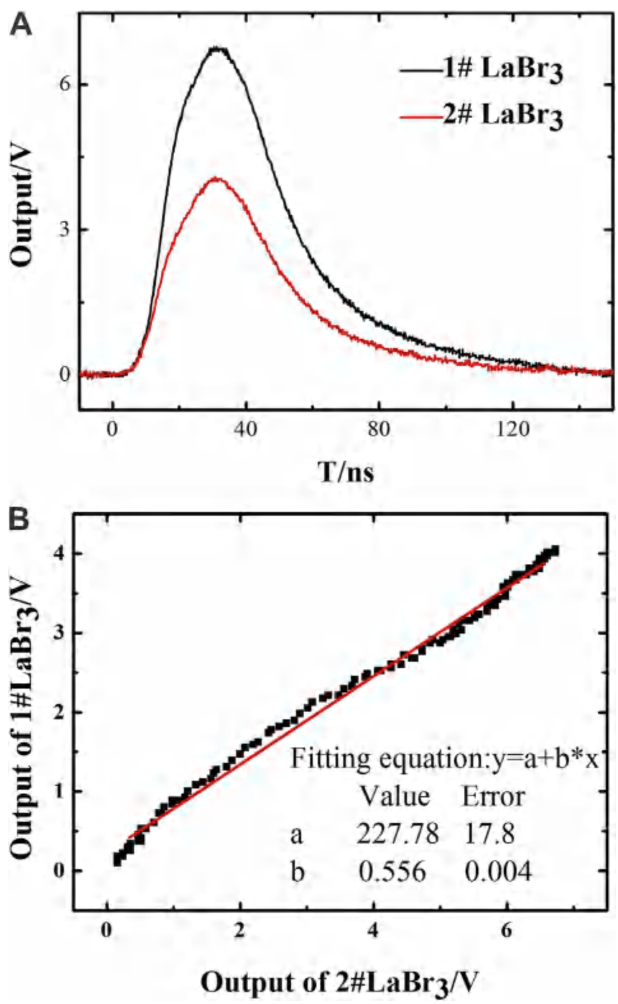

Fig. 5. Response of 2# $LaBr_3$ at a dose of 20.16 Gy.

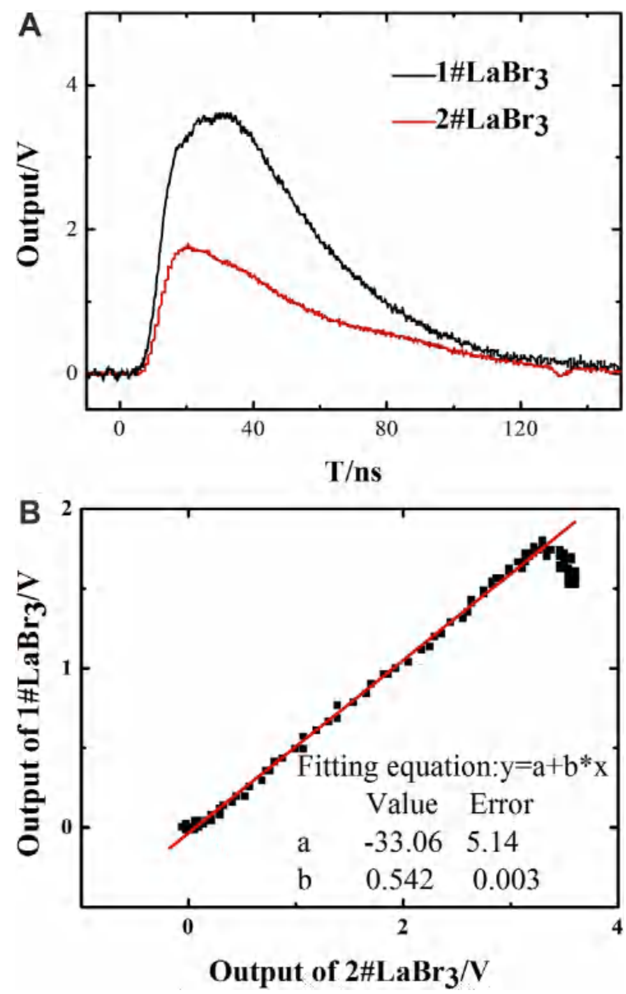

Fig. 6. Response of 2# $LaBr_3$ at a dose of 41.78 Gy.

dose that entered the latter detector was 0.002 Gy.

The nonlinear response of 1#$LaBr_3$ is shown in Fig. 6(b). The attenuation is 20 dB. The maximum output voltage of the former detector is 3.8 V according to Fig. 6 (b). The maximum output current of the former detector is 3.8 V × 10 × 4/50 Ω = 3.04 A which is less than the linear current I_{max} of the GD40 used in the former detector. It can be proved that the nonlinearity response was caused by light output nonlinearity of the $LaBr_3$ scintillator rather than photoelectric tubes. The dose that entered the former detector was 41.78 Gy and the dose that entered the latter detector was 0.005 Gy.

The response curves obtained for the first and second shots are shown in Fig. 7. The working condition of the plasma opening switch of the "QiangGuang-1″for each pulse is unstable. The secondary discharge or more discharges may happen during the discharge process which induces more peaks after the main peak.

The FWHM determined for the first shot was 25.1 ns. The FWHM determined for the second shot was 23.2 ns. The conversion formula for Gy/s and MeV/(cm^2·s) is: 1 Gy/s = 2.23 × 10^{11} MeV/(cm^2·s) (Su, 1982). The fluence rate for $LaBr_3$ in the first shot was 1.8 × 10^{20} MeV/(cm^2·s). The fluence rate for $LaBr_3$ in the second shot was 4.02 × 10^{20} MeV/(cm^2·s).

The reasons for fluence rate linear response limit of the $LaBr_3$ scintillator are the doping concentration of the luminescence centers (Ce^{3+}) and the process used for manufacturing the $LaBr_3$ scintillator. After X-rays hit $LaBr_3$, they deposit energy. Light is emitted then. The outputs of the $LaBr_3$ were almost proportional to the fluence rate under 1.8 × 10^{20} MeV/(cm^2·s). When the fluence rate was higher than 1.8 × 10^{20} MeV/(cm^2·s), some excited Ce^{3+} could escape the luminescence centers because of the high amount of energy deposited. This part of escaped Ce^{3+} changed a portion of deposited energy to thermal energy without light emission. (Yi et al., 2016).

3.2. Discussion

The saturated $LaBr_3$ scintillator was set at room temperature for 24 h before the next pulse. The former detector was set at the place where the fluence rate was no more than 1.8 × 10^{20} MeV/(cm^2·s). If the X-rays radiation damage is unrecoverable, the Lissajous figure is not a straight line. The result was shown in Fig. 8. The response was linear at a dose of 11.88 Gy. It can be concluded that the displacement of Ce^{3+} caused by high dose rate X rays was not permanent. The Ce^{3+} returned back to the centers after 24 h at room temperature. Thus, the saturated $LaBr_3$ scintillator can recover from radiation damage by the pulsed X-rays. This phenomenon was also observed in a study of radiation damage to $LaBr_3$ by gamma rays [Normand et al., 2007].

4. Conclusions

In this study, we measured the fluence rate linear response limits of $LaBr_3$ in experiments. The linear response limit of $LaBr_3$ was 1.8 × 10^{20} MeV/(cm^2·s) in a short X-ray pulse field. When using $LaBr_3$ scintillators in a high intensity pulsed radiation field, we recommend that the fluence rate into the scintillator should be less than 1.8 × 10^{20} MeV/(cm^2·s) to avoid inaccurate measurements due to a nonlinear response. Furthermore, the saturated $LaBr_3$ scintillator recovers from radiation

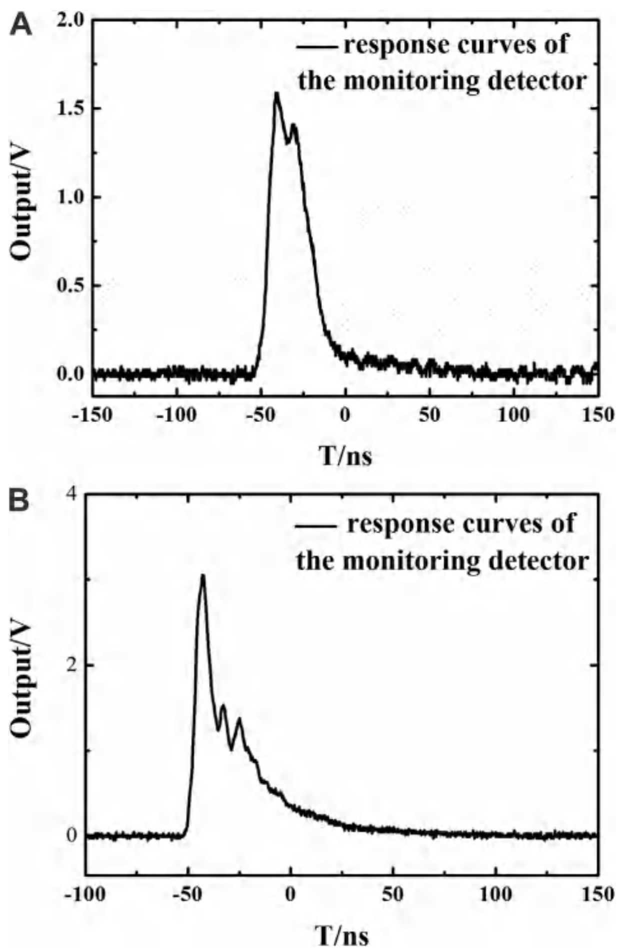

Fig. 7. Response curves obtained for the monitoring detector.

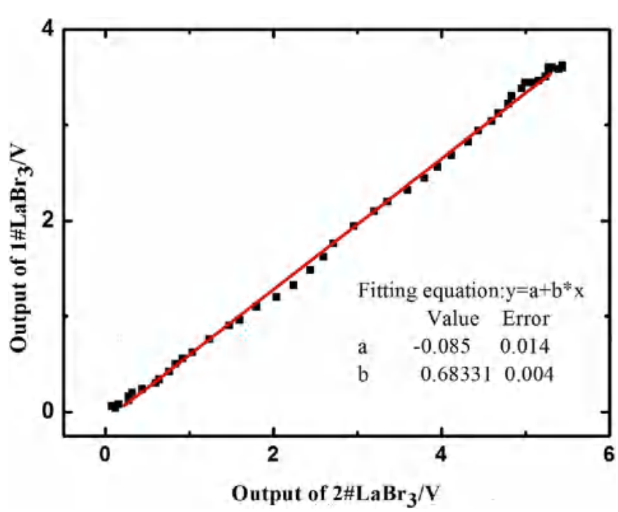

Fig. 8. Response of the saturated $LaBr_3$ tested after 24 h at a dose of 11.88 Gy.

damage by the pulsed X-rays after 24 h at room temperature which means the saturated $LaBr_3$ scintillator can recover spontaneously from radiation damage by the pulsed X-rays.

We infer that the main reasons for fluence rate linear response limit of the $LaBr_3$ scintillator are the doping concentration of the luminescence centers (Ce^{3+}) and the process used for manufacturing the $LaBr_3$ scintillator. The way of energy transmission between Ce^{3+} and scintillation materials and its efficiency are key factors, too. It remains to be studied further in the next work.

Acknowledgments

The authors thank researchers on the "QiangGuang-1" high power pulsed accelerator at Northwest Institute of Nuclear Technology for support with the experiments. This work was supported by the National Natural Science Foundation of China under Grants No. 11575146 and No. 11535010.

References

Cong, P., Chen, W., Han, J., et al., 2010. Analysis of measurement uncertainty of X-ray dose rate. High Power Laser Part. Beams 22 (11), 2773–2777.
Glodo, J., Moses, W.W., Higgins, W.M., et al., 2005. Effects of Ce concentration on scintillation properties of $LaBr_3$:Ce. IEEE Trans. Nucl. Sci. 52 (5), 1805–1808.
Guo, Z.Y., et al., 2014. The performance measurement study of Si-PIN nuclear radiation semiconductor detector. Nucl. Electron. Detect. Technol. 3, 414–418.
Krämer, K.W., Dorenbos, P., Güdel, H.U., et al., 2006. Development and characterization of highly efficient new cerium doped rare earth halide scintillator materials. J. Mater. Chem. 16 (27), 2773–2780.
Kuckuck, R.W., 1971. Semiconductor Detectors for Use in the Current Mode. Report of Lawrence Livermore National Laboratory, UCRL-51011. Lawrence Livermore National Laboratory, Livermore, CA, USA.
Kun-Sik Park, Park J.M., Yoon, Y.S., et al., 2006. Effects of the resistivity and crystal orientation of the silicon PIN detector on the dark current and radiation response characteristics. In: IEEE Nuclear Science Symposium Conference Record. IEEE, pp. 1068–1072.
Loef, E.V.D.V., Dorenbos, P., Eijk, C.W.E.V., et al., 2001. High-energy-resolution scintillator: Ce^{3+} activated $LaBr_3$. Appl. Phys. Lett. 79 (10), 1573–1575.
Loef, E.V.D.V., Dorenbos, L.P., Eijk, C.W.E.V., et al., 2002. Scintillation properties of $LaBr_3$:Ce^{3+} crystals: fast, efficient, and high-energy resolution scintillators. Nucl. Instrum. Meth. Phys. Res. 486 (1), 254–258.
Lu, Y., Song, Z.Z., Tan, X.J., et al., 2014. Performance of $LaBr_3$:Ce/$LaCl_3$:Ce scintillation detector in current mode. Atomic Energy Sci. Technol. 48 (1), 158–161.
Normand, S., Iltis, A., Bernard, F., et al., 2007. Resistance to γ irradiation of $LaBr_3$:Ce and $LaCl_3$:Ce single crystals. Nucl. Instrum. Meth. Phys. Res. 572 (2), 754–759.
Song, Z.H., Gang, L.I., Wang, K.L., et al., 2004. Testing the linear response of inorganic crystals at high dose rate. Nucl. Electron. Detect. Technol. 88 (3), 281–294.
Su, S.L., 1982. X-ray and Γ-ray Shielding Manual. Guizhou People Press, pp. 13–27.
Yi, Y.C., Song, Z.Z., Guan, X.Y., et al., 2016. Measurement of linear response upper limit of $LaBr_3$ to pulsed gamma radiation. High Power Laser Part. Beams 28 (9), 159–163.